American Journal of Engineering and Applied Sciences

Original Research Paper

Bi-Stable Vibration Power Generation System Using Electromagnetic Motor and Efficiency Improvement by Stochastic Resonance

[1]Wei Zhao, [2]Yoshiro Fujiwara, [2]Jingchao Guan, [2]Apollo B. Fukuchi and [2]Xilu Zhao

[1]Department of Research and Development, Space C5 Co., Ltd., Tokyo, Japan
[2]Department of Mechanical Engineering, Saitama Institute of Technology, Saitama, 369-0293, Japan

Article history
Received: 13-06-2023
Revised: 13-06-2023
Accepted: 25-06-2023

Corresponding Author:
Jingchao Guan
Department of Mechanical Engineering, Saitama Institute of Technology, Saitama, 369-0293, Japan
Email: guanjingchao123@gmail.com

Abstract: Research on vibration energy harvesting using stochastic resonance has become an important research topic. A vibration energy harvesting system was developed using electromagnetic motors based on an obliquely supported bistable motion model consisting of a spring mass. After formulating the motion-governing equations of the proposed vibrating system and analyzing its potential energy performance, it was demonstrated that the system exhibits bi-stable vibration characteristics throughout its entire range of motion. To expand the vibration amplitude using the stochastic resonance phenomenon, a prediction formula for the periodic excitation frequency that causes stochastic resonance was derived using Kramer's rate. An experiment was conducted; the obtained results and predicted values of the excitation frequency agreed well and the validity of the prediction formula for the periodic excitation frequency of stochastic resonance was verified. It was confirmed that the proposed bistable vibration energy harvesting system reliably generated stochastic resonance by exciting random and periodic signals at the same time. The results of the experiment indicate that there was a significant vibration amplification effect, which significantly improved the vibration power generation performance.

Keywords: Vibration Energy Harvesting, Bi-Stable Vibration System, Stochastic Resonance, Nonlinear Vibration System, Vibration Power Generation

Introduction

With the development and widespread use of renewable energy, research on vibration energy harvesting has gained attention and a large amount of research results have been published (Zhang *et al*., 2018a; Stephen, 2006; Khan and Ahmad, 2016). Vibration energy harvesting is a power generation method for converting mechanical vibration into electrical energy. The amount of generated power increases with the increase in vibration amplitude. An important issue is how to develop a vibrating device with a large amplitude.

Conventionally, the natural frequency of a vibrating system is tuned to match the frequency of the environmental vibrations. Vibration energy harvesting has been studied by increasing the amplitude of a vibrating system through the generation of resonance phenomena (Lallart *et al*., 2010; Kubba and Jiang 2013; Dong *et al*., 2015). However, there are some vibration environments with single frequencies; thus, achieving continuous large amplitudes is not possible.

To overcome this limitation, a proposed approach involves installing multiple vibration models with distinct natural frequencies within a single vibration system. However, it has been reported that this approach is difficult to apply because the required equipment is large and complicated (Chen *et al*., 2019; Dai, 2016). To address this problem, nonlinear vibration systems for applications to vibration environments containing multiple frequency components have been proposed. However, because the vibration amplitudes are still small, the approach is difficult to apply to develop vibration energy harvesting systems (Yang and Towfighian, 2017; Gafforelli *et al*., 2014; Gammaitoni *et al*., 2009).

Hence, there is a proposal for conducting research and development on novel vibration energy harvesting systems that leverage stochastic resonance phenomena. Stochastic resonance phenomena can remarkably increase

the vibration amplitudes of bistable vibration models in random vibration environments. Stochastic resonance refers to a physical phenomenon where the addition of a weak periodic signal to a nonlinear system, subjected to random excitation, can significantly amplify the response signal under specific probabilities. Many theoretical studies have been published to elucidate stochastic resonance (Gammaitoni *et al*., 1998; Benzit *et al*., 1981; McNamara and Wiesenfeld, 1989; Tretyakov, 1998; Rosas and Lindenberg, 2016).

In mechanical systems, by adding a periodic signal to a bi-stable vibrating system receiving a random excitation signal, the response vibration of the system can be substantially amplified. The stochastic resonance phenomena obtained in this manner are used to generate vibration power (Harne and Wang, 2013; Pellegrini *et al*., 2013; Yao *et al*., 2011). Thus, the development of bi-stable vibration systems that can generate stochastic resonances for mechanical systems is important.

Currently, most of the research on bistable vibration systems in mechanical systems utilize cantilever beams with mass blocks attached to their ends (Li *et al*., 2020; Wang *et al*., 2019; Ibrahim *et al*., 2017; Kumar *et al*., 2018; Ali *et al*, 2011; Friswell *et al*., 2012; Lan and Qin, 2014; Bilgen *et al*., 2015). Also, significant work has been done to improve the performance of bistable oscillation. A bistable vibration model combining parallel beams from multiple cantilevers has been proposed (Zhou *et al*., 2015; Gao *et al*., 2016; Lan *et al*., 2018). A bistable vibration model with the modified internal geometry of a thin cantilever has been proposed (Zhang *et al*., 2018b; Podder *et al*., 2015; Bouhedma *et al*., 2019). A bi-stable vibration model consisting of a laterally bent beam structure has been proposed (Cottone *et al*., 2014; Liu *et al*., 2013a-b). A tristable vibration model has been proposed by changing the number of magnets attached to the tip of the cantilever and its vicinity (Zou *et al*., 2017; 2018; Mei *et al*., 2020a-b; Cao *et al*., 2015).

In practical applications of vibration energy harvesting, it has been commonly observed that bi-stable vibration models of mechanical systems, in their natural vibration environments, tend to vibrate with relatively low amplitudes due to random excitation signals. The applications of periodic excitation signals to bi-stable vibration models for the generation of stochastic resonance phenomena and the use of substantially amplified bi-stable vibrations are promising research topics.

Consequently, a bi-stable vibration model was developed by utilizing a cantilever beam with a magnet affixed to its tip. Subsequently, an investigation was carried out to explore the stochastic resonance phenomenon within this bi-stable model (Zheng *et al*., 2014). In addition, the usefulness of bi-stable vibration energy harvesting systems suitable for implementation in vehicle tires has been evaluated (Zhang *et al*., 2015).

Using cantilevers for vibration power generation results in stable vibration. The structures of cantilevers are difficult to cope with accidental disturbance loads and large-scale vibration models capable of more stable vibrations are required (Zuo and Tang, 2013).

Therefore, a large-scale bi-stable motion model composed of springs and mass blocks was proposed. Bi-stable motion systems that can generate stochastic resonance more reliably than conventional bi-stable vibration systems and secure large amplitude have been developed (Zhao *et al*., 2020). An electromagnetic induction vibration power generation method, which uses magnets and coils, has been studied as a replacement for the conventional piezoelectric method (Zhao *et al*., 2022a-b).

However, the high center of gravity of the vibration energy harvesting system has low stability. Therefore, horizontally-opposed bi-stable vibration energy harvesting systems have been proposed and studied for application in low installation space conditions (Guo *et al*., 2022a-b).

However, the low efficiency of vibration power generation and low stability of vibration systems in random vibration environments have not been solved.

In this research, we designed a novel vibration energy harvesting system using a horizontal bi-stable motion model comprising elastic springs and mass blocks. Additionally, a commercially available electromagnetic motor was incorporated into the system. It was demonstrated that the system exhibits bi-stable vibration characteristics throughout its entire range of motion, by establishing the governing equations of the moving body and analyzing the potential energy distribution of the vibration system. To effectively utilize the stochastic resonance of a bi-stable vibration system, we derived a predictive formula for the periodic excitation frequency, where stochastic resonance is most likely to occur. We conducted vibration experiments on a verification experimental device for bi-stable vibration energy harvesting systems, utilizing both random and periodic excitation signals. The measurement results were then analyzed to investigate the vibration amplification effect and the electricity generation from vibration power due to the occurrence of stochastic resonance.

Materials and Methods

Bi-Stable Vibration Harvesting System

A bi-stable vibration energy harvesting model was developed, as shown in Fig. 1. Four identical electromagnetic motors were mounted below a mass block above a horizontal rail. When the mass block moved left and right, the electromagnetic motor rotated through the gear and an AC voltage was outputted from the lead wire of the motor.

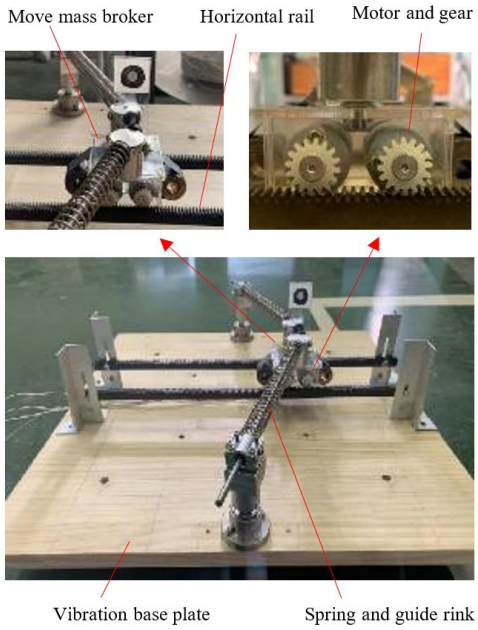

Fig. 1: Experimental setup for the horizontal bi-stable vibration energy harvesting

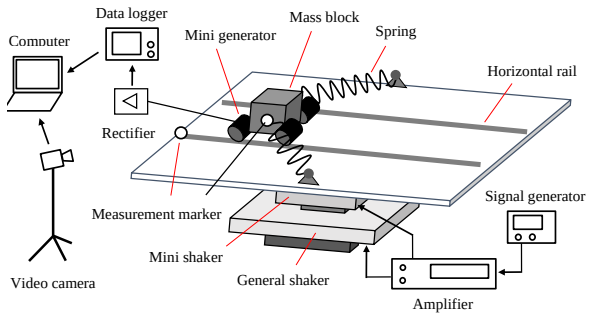

Fig. 2: Measurement system for the bi-stable vibration energy harvesting

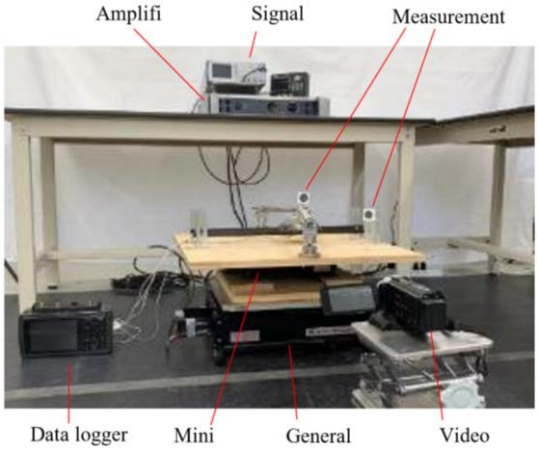

Fig. 3: Experimental device for bi-stable vibration harvesting system

Table 1: Details of the experimental setup

Items	Brands and parameters
Mass block weight	800 g
Horizontal rail	Length 500 mm
Vertical distance	Distance from a pin support point to rail 180 mm
Elastic spring	Spring coefficient 175 N/m, initial length 250 mm
Mini shaker	SSV-105 (SAN ESU Co. Ltd)
General shaker	SSV-125 (SAN ESU Co. Ltd)
Amplifier	SVA-ST-30 (SAN ESU Co. Ltd), 2 Channel
Video camera	GZ-E765 (JVC Co. Ltd)
Function generator	NF-WF1973 (NF corporation)
Mini-function generator	JDS2800 (Hangzhou measurement instrumentation Co.)
Data logger	GL2000 (Graphtec corporation)
Marker tracking software	MOVIS Neo V3.0 (NAC image technology Inc.)

To give excitation conditions, the bi-stable vibration power generation experimental device was installed on a mini shaker, which was installed on a general shaker. During the experiment, the general shaker was used to generate random signal excitations to simulate a natural environment, and the mini shaker was used to generate periodic stimulus signal excitations to induce stochastic resonance. Thus, the stochastic resonance effect was investigated using the mini and general shakers for independent or joint excitation.

To determine the results of the experiment, a high-speed camera was used to photograph the measurement markers attached to the mass block and support base, as shown in Fig. 2. The recorded data was read using a personal computer and time-series data of the vibration displacement was generated using tracking software. A data logger was employed to capture and record the oscillating voltage produced in the coil. In this case, because the phases of the output voltages of the four electromagnetic motors were different, the AC voltage was rectified into a DC voltage using a diode rectifier circuit and then connected to a data logger to record the voltage levels of the generated vibration power. Figure 3 shows a photograph of the fabricated experimental device and Table 1 lists its configuration specifications.

Vibration Characteristics of Bi-Stable Systems

The main components of the proposed vibration model are shown in Fig. 4(a). m is the mass of the mass block, x_d is the distance from the axis of symmetry of the mass block and x_t is the distance from the axis of symmetry of the support point. F is the elastic force of the spring and F_c is the damping force owing to kinetic friction. h is the vertical distance from the support point to the center point of the mass block and θ is the angle between the spring and horizontal axes.

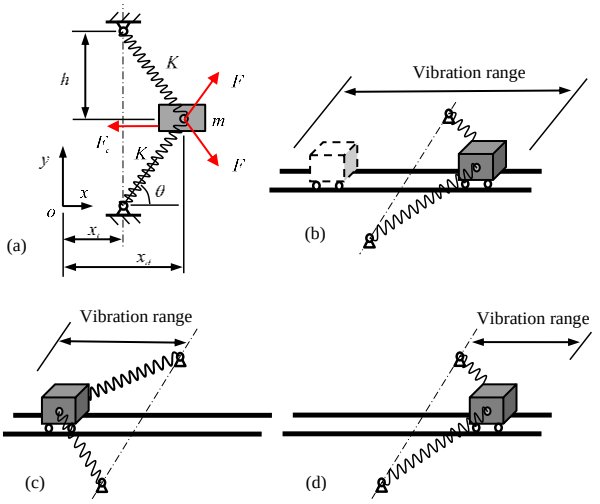

Fig. 4: Analysis model and vibration state of the bi-stable vibration system

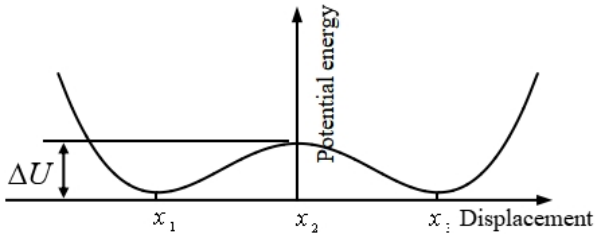

Fig. 5: Distribution of potential energy with a displacement of the mass block

However, the initial length l_0 of the elastic spring was longer than the distance h. The mass block exhibited three vibration states and had one static equilibrium position on each side of the axis of symmetry, as depicted in Fig. 4(b-d). Figure 4(c-d) show the mono-stable oscillations and Fig. 4(b) shows the bi-stable oscillations (Guo *et al*., 2022a).

In a real-world random vibration environment, a mono-stable vibration system experiences significant amplification when the mass block receives periodic excitation and crosses the peak of potential energy at the center. This study utilized this amplification characteristic.

Based on Fig. 4(a), the equation of motion of the mass block along the direction can be expressed as follows:

$$m\ddot{x}_d + c\left(\dot{x}_d - \dot{x}_t\right) + 2F\cos\theta = 0 \tag{1}$$

where, c is the damping coefficient. Elastic force and tilt angle were calculated using the following equations:

$$F = K\left(\sqrt{\left(x_d - x_t\right)^2 + h^2} - l_0\right) \tag{2}$$

$$\cos\theta = \frac{x_d - x_t}{\sqrt{\left(x_d - x_t\right)^2 + h^2}} \tag{3}$$

where, K is the spring constant. Substituting Eqs. (2-3) into Eq. (1), the equation of motion is expressed as follows:

$$m\ddot{x}_d + c(\dot{x}_d - \dot{x}_t) + 2K(1 - \frac{l_0}{\sqrt{(x_d - x_t)^2 + h^2}}(x_d - x_t) = 0 \tag{4}$$

Here, the relative distance between the mass block and the support point can be expressed as follows:

$$x = x_d - x_t \tag{5}$$

Substituting Eq. (5) into Eq. (4), the equation of motion for relative displacement is expressed as follows:

$$m\ddot{x} + c\dot{x} + 2K\left(1 - \frac{l_0}{\sqrt{x^2 + h^2}}\right)x = -m\ddot{x}_t \tag{6}$$

Equation (6) indicates that a damping force is generated because of friction. To determine the characteristics of the potential energy of the vibration model, the potential energy is expressed by the following equation based on the motion governing Eq. (6):

$$U = Kx^2 - 2Kl_0\sqrt{x^2 + h^2} \tag{7}$$

To investigate the distribution characteristics of the potential energy, the extreme value of the equation was obtained by differentiating with respect to Eq. (7):

$$K\left(1 - \frac{l_0}{\sqrt{x^2 + h^2}}\right)x = 0 \tag{8}$$

Solving Eq. (7) resulted in the following:

$$x_1 = \sqrt{l_0^2 - h^2}\ \ x_2 = 0\ \ x_3 = \sqrt{l_0^2 - h^2} \tag{9}$$

x_1, x_2, and x_3 in Eq. (9) are the extreme values of the potential energy and correspond to the rest equilibrium positions of the mass block.

The potential energy values obtained using Eq. (7) were plotted in Fig. 5, where x_1, x_2, and x_3 correspond to the extreme values of the potential energy obtained using Eq. (9). Troughs x_1 and x_3 are the centers of two monostable vibrations on the left and right and peak x_2 is the center of the bi-stable vibration located at the central axis of symmetry. ΔU is the barrier value between the left and right bistable oscillations.

A bi-stable vibration model in a random vibration environment generally exhibits monostable vibration. Nonetheless, when random and periodic signals coexist, they induce bi-stable vibration, resulting in a resonance phenomenon where the vibration displacement experiences significant amplification. This particular resonance phenomenon is termed stochastic resonance, as it involves uncertain factors arising from the random excitation environment (Guo *et al*., 2022a).

The local equivalent stiffness was determined at the stable vibration points on both sides of the bi-stable vibration model, as well as at the unstable vibration point located at the center can be expressed by the following equations:

$$K_a = U''\left(\sqrt{l_0^2 - h^2}\right) \tag{10}$$

$$K_0 = U''(0) \tag{11}$$

where, K_a is the local equivalent stiffness at the stable vibration points on both sides and K_0 is the local equivalent stiffness at the stable vibration point on the central axis of symmetry.

Using Eqs. (7, 10, and 11), ignoring frictional damping effects, the equivalent natural frequency f_a at the stable points on either side of the bi-stable system and the central instability the equivalent natural frequency f_0 at the vibration point can be calculated using the following equations:

$$f_a = \frac{1}{2\pi}\sqrt{\frac{K_a}{m}} = \frac{1}{2}\sqrt{\frac{2K}{m}\left(1 - \frac{h^2}{l_0^2}\right)} \tag{12}$$

$$f_0 = \frac{1}{2\pi}\sqrt{\frac{K_a}{m}} = \frac{1}{2\pi}\sqrt{\frac{2k}{m}\left(\frac{l_0^2}{h} - 1\right)} \tag{13}$$

The configuration parameters of the bi-stable oscillatory system listed in Table 1 were substituted into Eqs. (12-13). The equivalent natural frequencies at the stable vibration points on both sides of the bistable vibration system and those at the central unstable vibration point were obtained as follows:

$$fa = 2.310Hz \tag{14}$$

$$f_0 = 2.076Hz \tag{15}$$

Prediction of Frequency at Which Stochastic Resonance Occurs

The periodic excitation frequency at which the stochastic resonance phenomenon of the bistable vibration system was most likely to occur was determined using Kramer's rate value, as follows (Gammaitoni *et al*., 1998):

$$f_k = \frac{w_a w_0}{4\pi q} exp\left(-\frac{\Delta\bar{U}}{D}\right) \tag{16}$$

where, w_a and w_0 are the equivalent natural vibration angular frequencies at the stable and unstable equilibrium points, respectively, $\Delta\bar{U}$ is the potential energy barrier value, q is the damping coefficient corresponding to the motion unit mass and D is the random signal strength.

For the bi-stable oscillation system of this study, w_a, w_0, $\Delta\bar{U}$ and q were calculated using the following equations:

$$w_a = \sqrt{\frac{2K}{m}\left(1 - \frac{h^2}{l_0^2}\right)} \tag{17}$$

$$w_0 = \sqrt{\frac{2K}{m}\left(\frac{l_0}{h} - 1\right)} \tag{18}$$

$$\Delta\bar{U}\frac{1}{m}\left[U(0) - U\sqrt{\left(l_0^2 - h^2\right)}\right] = \frac{K}{m}(l_0 - h)^2 \tag{19}$$

$$q = \frac{c}{m} \tag{20}$$

Substituting Eqs. (17-20) into Eq. (16), the frequency of the periodic signal at which the stochastic resonance of the bi-stable oscillation system in this study would likely occur is expressed by the following equation:

$$f_k = \frac{K\left(l_0 - h\right)}{2\pi q l_0}\sqrt{\frac{l_0 + h}{h}}\exp\left(-\frac{K(l_0 - h)^2}{mD}\right) \tag{21}$$

Here, the damping coefficient c = 2.36 Ns/m was obtained by assigning an initial displacement to the mass block and measuring the free damping motion displacement. Random signal strength D = 1.65 J/Kg was obtained through a calculation using the response displacements of the support base measured when only the random signal was excited.

After substituting the configuration parameters of the bi-stable vibration system from Table 1 into Eq. (21), the resulting periodic excitation frequency at which stochastic resonance is most likely to occur is as follows:

$$f_k = 2.134Hz \tag{22}$$

Equations (14, 15 and 22) indicate that the periodic excitation frequency at which the stochastic resonance of the bi-stable system was most likely to occur was between the natural frequencies of the stable and unstable vibration points.

Results and Discussion

For investigative purposes, we conducted measurement experiments for three experimental cases: (1) Excitation with a random signal, (2) Excitation with a periodic signal, and (3) Simultaneous excitation with both signals.

The periodic frequency used in the measurement experiment ranged from 1.2-3.2 Hz at intervals of 0.5 Hz with reference to the predicted excitation frequency described in Eq. (22). The amplitude of the periodic excitation signal was uniformly set at 20 mm.

There were many cases in which the response displacement of the bi-stable vibration system used in this study had a random distribution. To quantitatively evaluate the amplification effect of stochastic resonance, the standard deviation of vibration displacement calculated using the following formula was used as an evaluation index for vibration displacement:

$$S = \sqrt{\frac{1}{N}\sum_{i=1}^{N}(x_i - \bar{x})^2} \tag{23}$$

where, x_i represents the measured vibration displacement, $\bar{x}$ is the average vibration displacement and N is the total number of sampled vibration displacement values in the time series.

The efficiency of vibration power generation was evaluated by calculating the amount of electric power generated using the following formula:

$$S = \sqrt{\frac{1}{N}\sum_{i=1}^{N}x_i - \bar{x})^2} \tag{24}$$

where, $V_{\text{exp } er\text{-}i}$ represents the measured voltage in the vibration experiment at each sampling point, N is the total time steps, Δt is the time step size, T is the total duration of the measurement and R is the electrical resistance of the measurement circuit.

In the experiment, the total measurement time T = 60 s, the step time width Δ t = 0.01 s, and the total number of steps N = 6000. The electrical resistance of the measuring circuit was the same as the electrical resistance of the generator motor coil, thus R = 135 Ω .

Figures 6-16 show the results of each excitation experiment. Each Fig. (6-16a) shows the vibration displacements, where the red line indicates the vibration displacement of the mass block and the blue line indicates the vibration displacement of the support point. Each Fig. (6-16b) shows the generated electrical power of the vibration power generation system. Each Fig. (6-16c) shows the vibration phase diagram represented by the velocity and displacement of the mass block. Each Fig. (6-16d) shows the vibration phase diagram represented by the velocity and displacement of the supporting point.

Excitation with Random Signal

Figure 6 shows the measured excitation with only random signals. According to Fig. 6, under the excitation of only random signals, the vibration displacement remained relatively small, and the motion of the mass block initiated from the left side. It exhibited random monostable motion on the left side of the axis of symmetry. The standard deviations of the vibration displacements for the mass block and support point were 10.86 mm and 9.81 mm, respectively, while the electrical power generated by the vibration power generation system was 0.01 W.

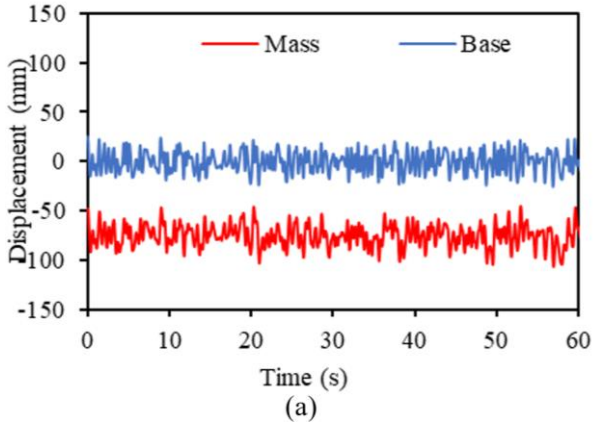

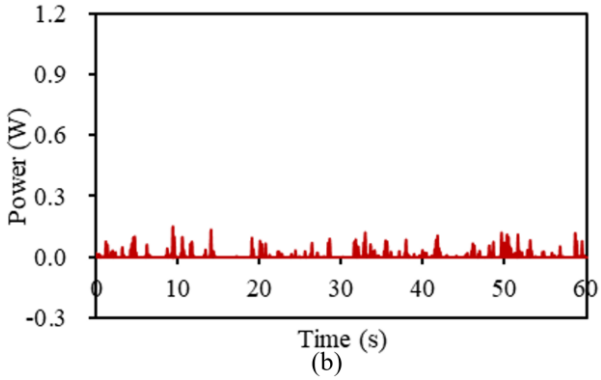

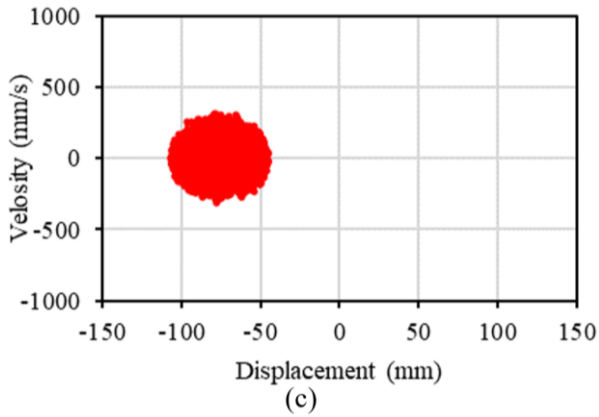

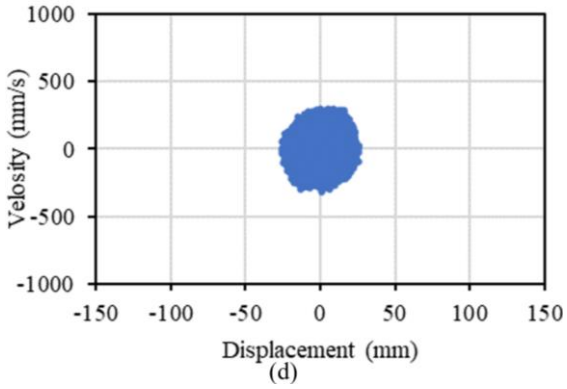

Fig. 6: Vibration power generation measurement result excited by a random signal

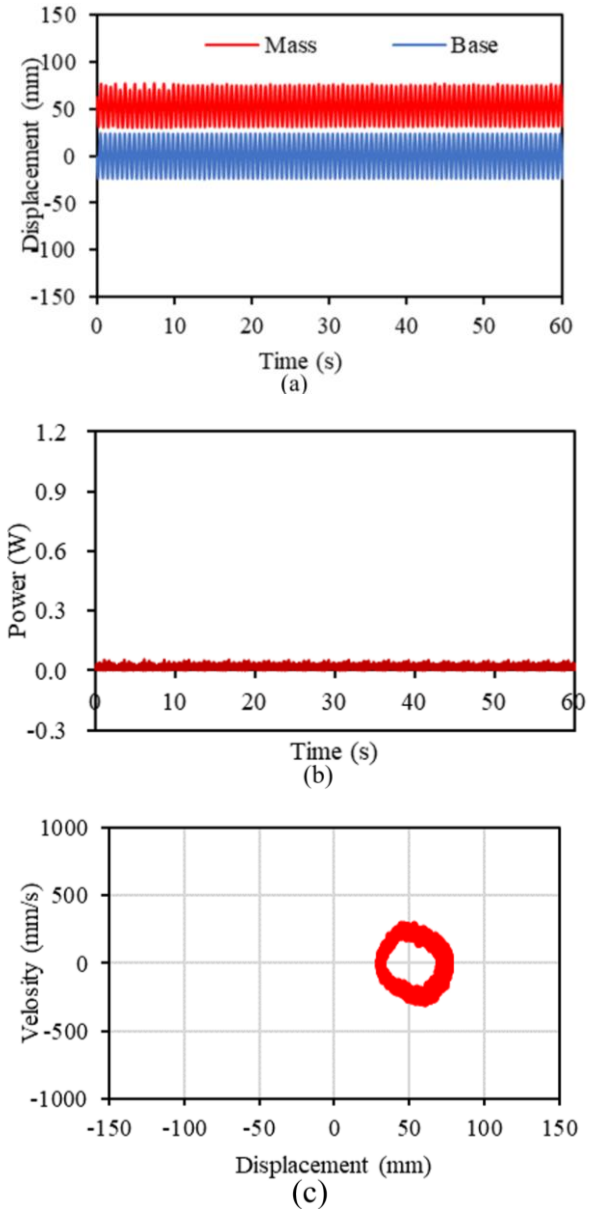

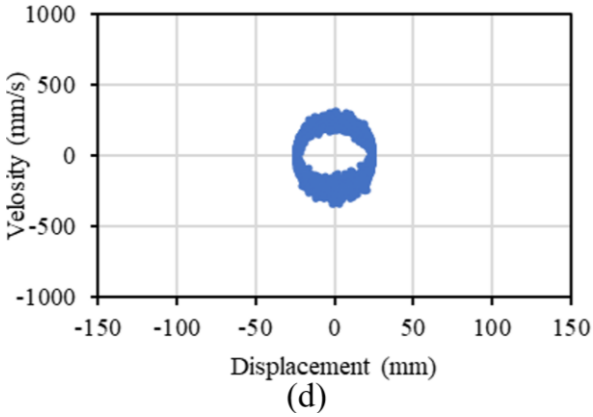

Fig. 7: Vibration power generation measurement result excited by period signal 1.2 Hz

Excitation Using Periodic Signals

Figures 7-11 show the measured periodic signal excitation at frequencies ranging from 1.2-3.2 Hz and the periodic characteristics of the vibration response displacement were confirmed. Because the bi-stable vibration system had nonlinear characteristics, as shown in Eq. (6), the shape of the vibration response displacement was slightly different from a simple sine wave. The distribution of the electrical power of the vibration power generation system was uniform.

Figures (7-11a) indicate that the mass block exhibited monostable vibration on the right side because the mass block began to move from the right side. As the vibration frequency increased, the frequency of the vibration response of the mass block increased and the vibration amplitude tended to decrease slightly. The excitation frequency was constant, and the vibration response amplitude of the mass block was almost constant; thus, the vibration time increased, and the electrical power of the vibration power generation system under periodic excitation did not appear to be major changes and was relatively stable. However, as the vibration frequency increased, the generated electrical power tended to increase gradually.

Figures (7-11c) show that the vibration response of the mass block had a ring shape with periodic vibration characteristics and exhibited monostable vibration on the right side. In addition, it was confirmed that the amplitude gradually decreased as the periodic excitation frequency increased, but the speed pick value did not change substantially. Figures (7-11d) show that the vibration response of the support point had a ring shape with periodic vibration characteristics and exhibited monostable vibration around the central point. It was observed that the amplitude value gradually decreased as the periodic excitation frequency increased.

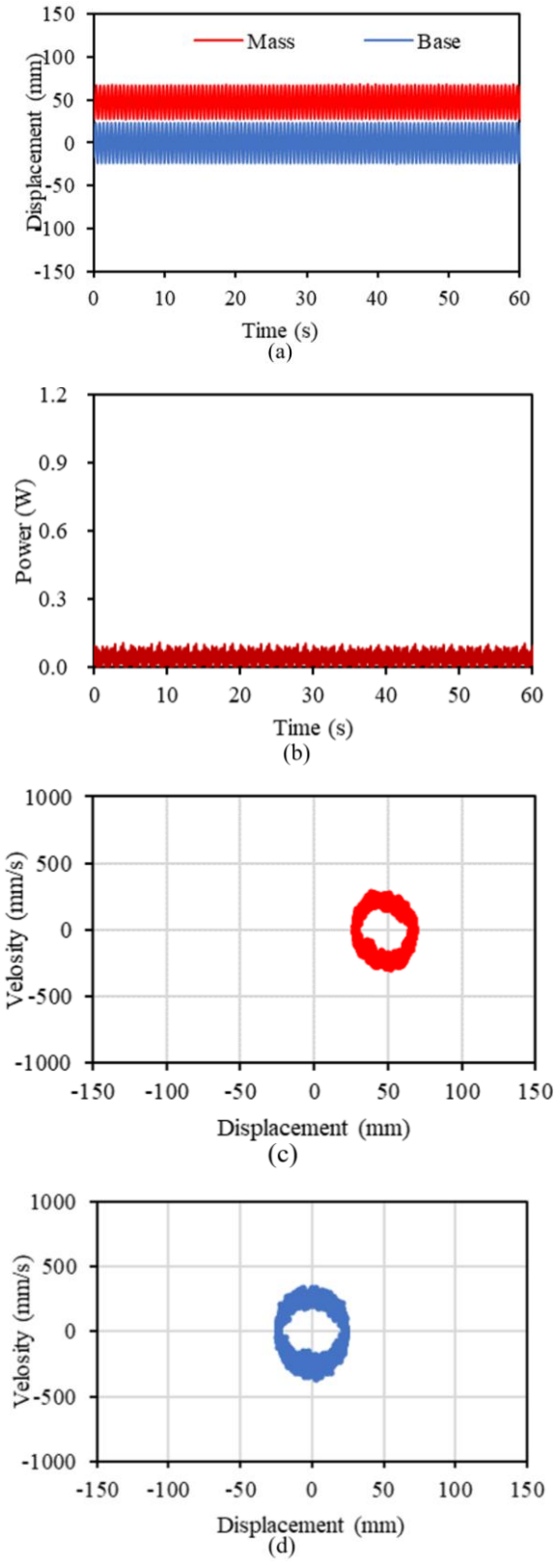

Fig. 8: Vibration power generation measurement result excited by period signal 1.7 Hz

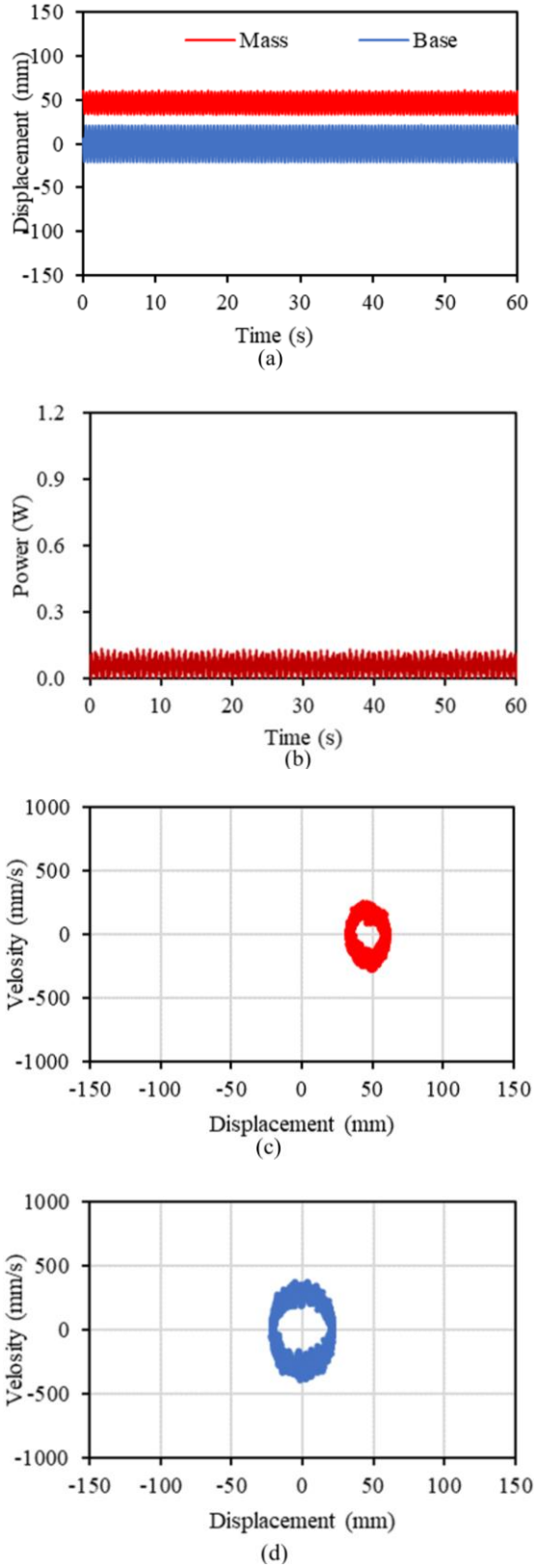

Fig. 9: Vibration power generation measurement result excited by period signal 2.2 Hz

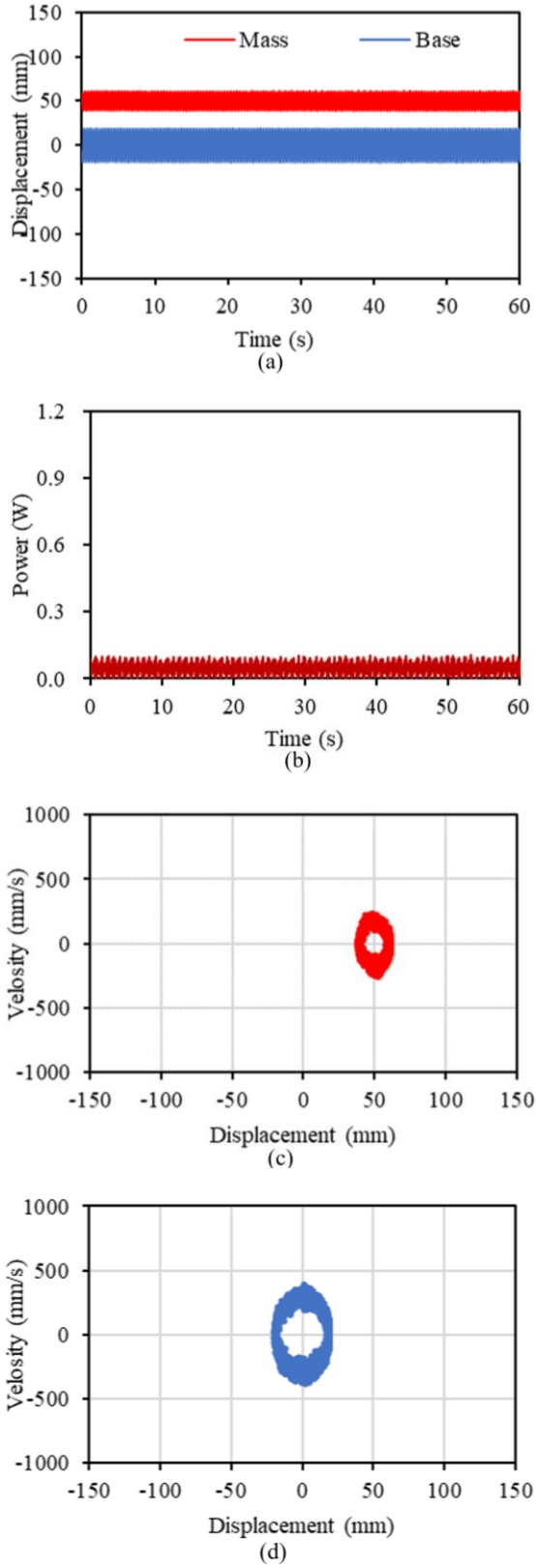

Fig. 10: Vibration power generation measurement result excited by period signal 2.7 Hz

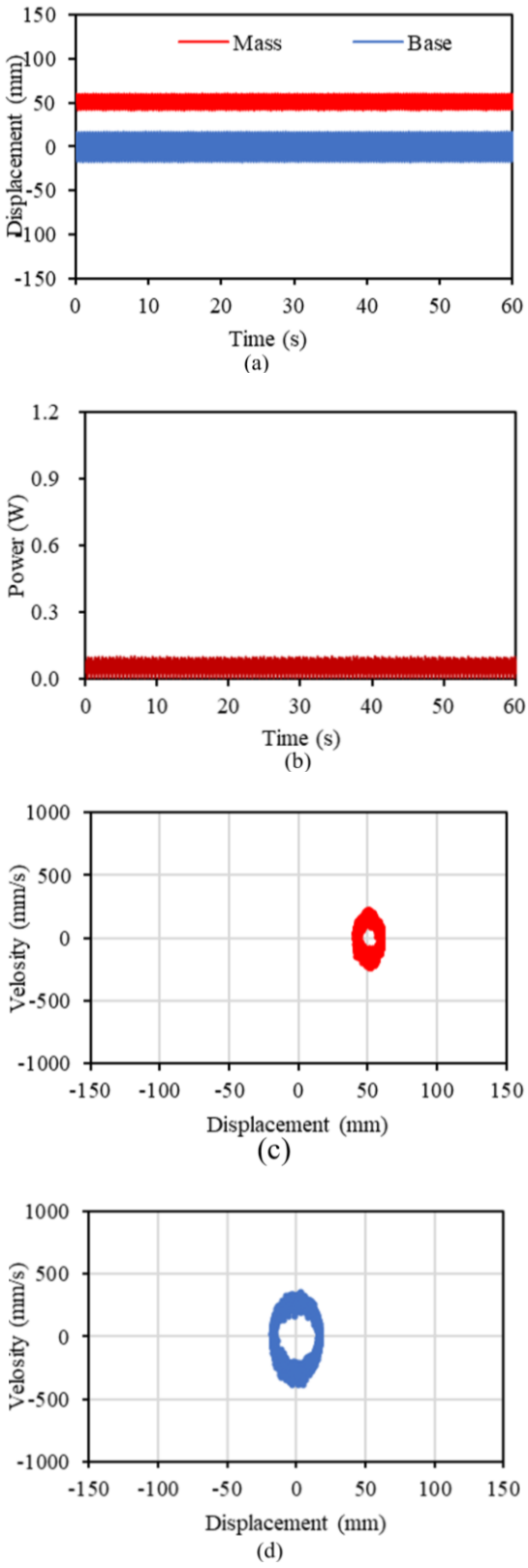

Fig. 11: Vibration power generation measurement result excited by period signal 3.2 Hz

Excitation Using Random and Periodic Signals

Figures 12-16 show the results of joint excitation using random and periodic signals. It was observed that the vibration response of the mass block changed substantially with the change in the excitation frequency. With the periodic signal set at 1.2 Hz, the vibration response displacement distribution in Fig. 12(a) reveals that the vibration displacement of the mass block was slightly greater than that of the support point; thus, there was no monostable motion. The electrical power of the vibration power generation system was randomly distributed, as shown in Fig. 12(b); the maximum electrical power was 0.4 W. Figure (12c-d) show that the vibration response of the mass block was larger than the periodic excitation and exhibited continued monostable vibration.

When the frequency of the periodic signal was set to 1.7, 2.2, and 2.7 Hz, the vibration of the mass block was relatively violent and the mass block vibrated, as shown in Figs. (13-15a). It was observed that the vibration of the mass block changed from monostable to bi-stable motion and stochastic resonance phenomenon began to occur. Therefore, it was confirmed that the electrical power generated from vibration was higher than that generated from periodic excitation, as shown in Figs. (13-15b). Figures (13-15c) show that the vibration response of the mass block was bistable. Figures (13-15d) show that the vibration response of the support point was continued monostable vibration with the center as the central point.

When the periodic signal was 3.2 Hz, the vibration of the mass block became smaller and the bi-stable motion phenomenon disappeared, as shown in Fig. 16(a), resulting in a monostable motion state. The electrical power of the vibration power generation system decreased, as shown in Fig. 16(b). Figures (16c-d) show that the vibration responses of the mass block and the support point were continued monostable vibrations.

Amplification Effect of Stochastic Resonance

The response displacement of the support point, which received an excitation signal, served as the reference for comparison. The standard deviations of the response displacements for both the mass block and support point were calculated using Eq. (23), and the stochastic resonance effect was evaluated using the ratio described in the following equation:

$$S_{ratio} = \frac{S_{mass}}{S_{base}} \tag{25}$$

where, S_{mass} and S_{base} are the standard deviations of the response displacements of the mass block and support point, respectively. The standard deviation for each experimental response displacement obtained in the previous section was calculated using Eq. (25) and the results are shown in Fig. 17.

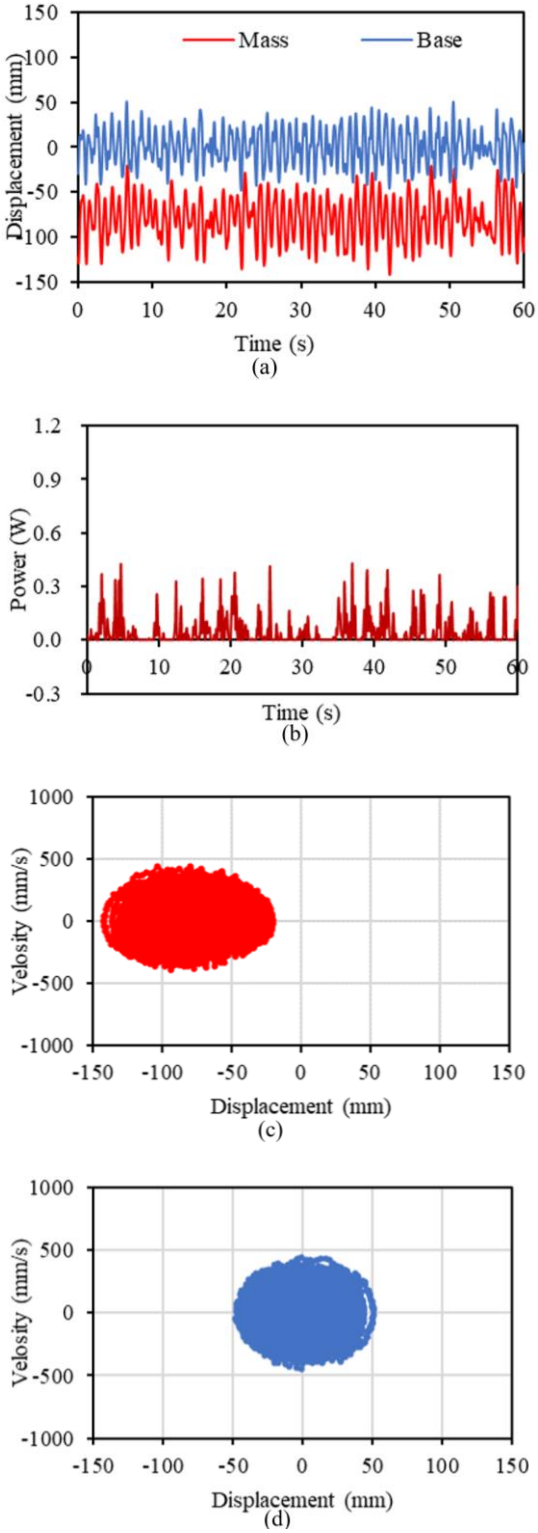

Fig. 12: Vibration power generation measurement result excited by random and period signal 1.2 Hz

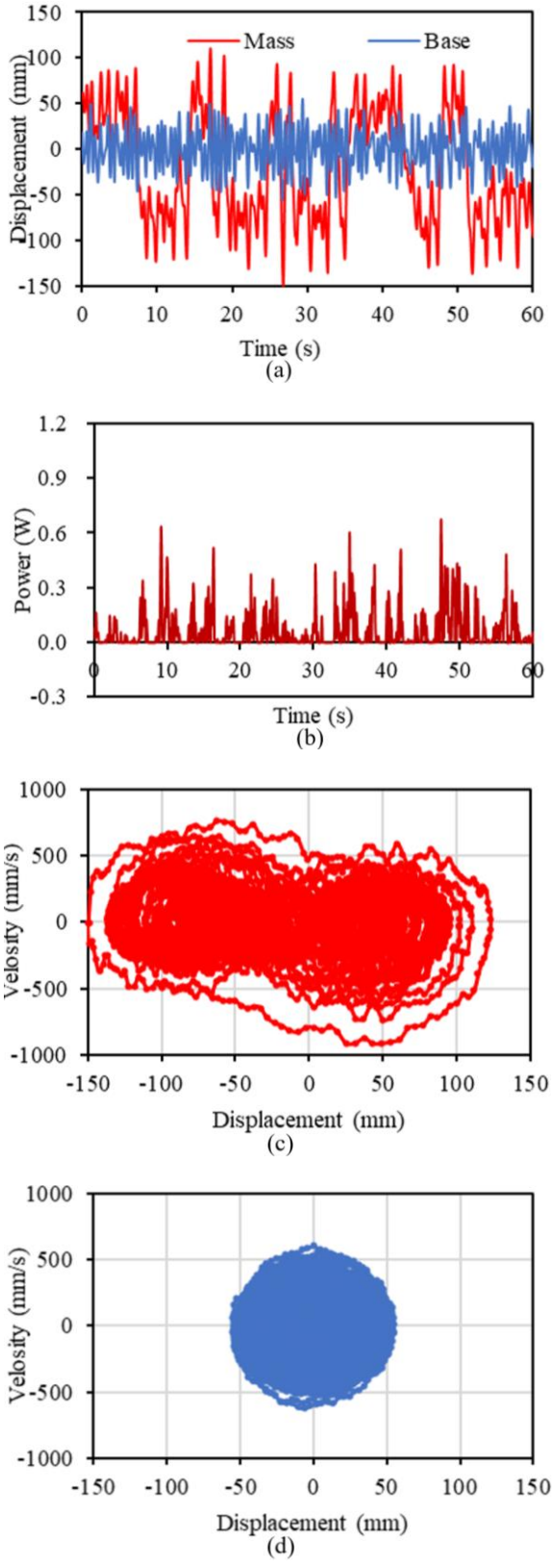

Fig. 13: Vibration power generation measurement result excited by random and period signal 1.7 Hz

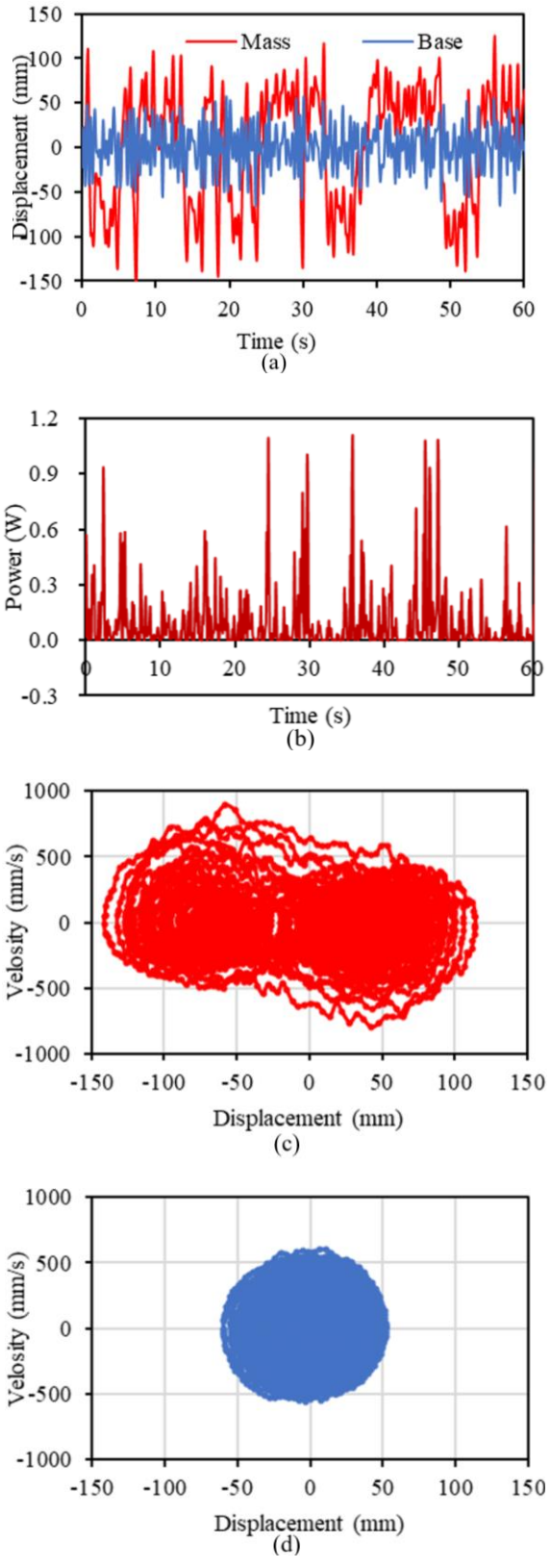

Fig. 14: Vibration power generation measurement result excited by random and period signal 2.2 Hz

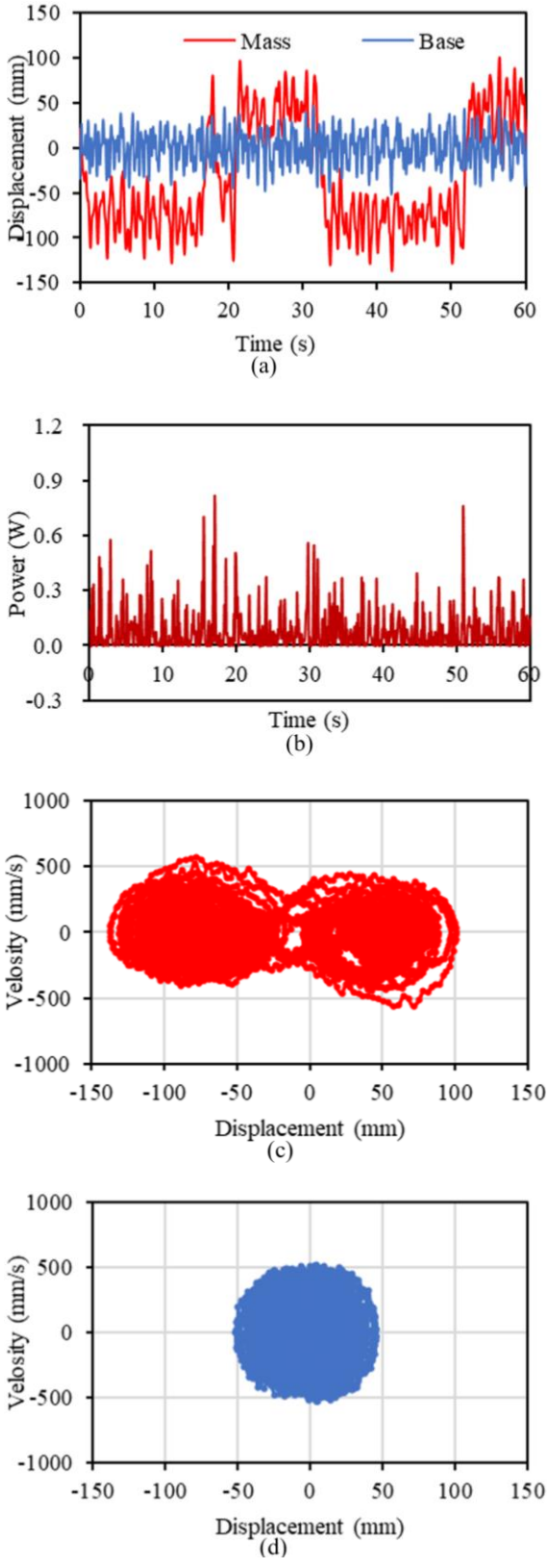

Fig. 15: Vibration power generation measurement result excited by random and period signal 2.7 Hz

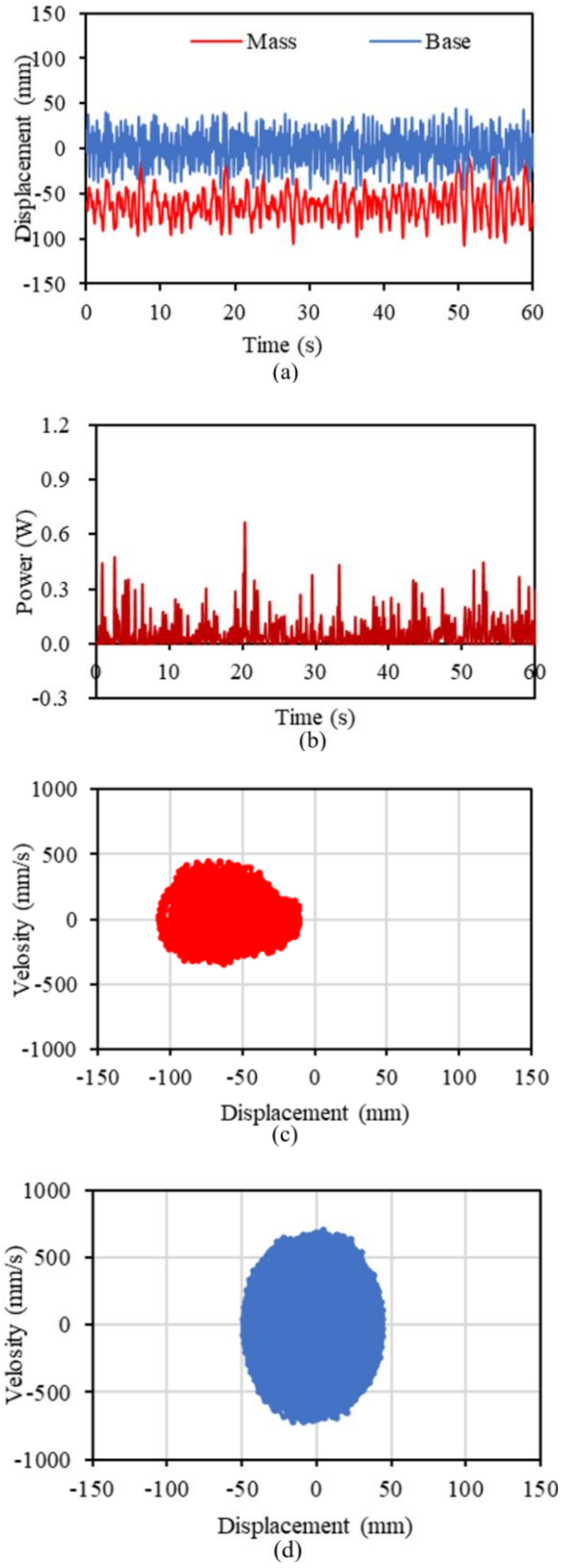

Fig. 16: Vibration power generation measurement result excited by random and period signal 3.2 Hz

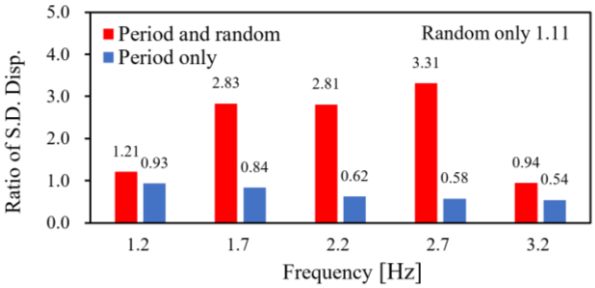

Fig. 17: Amplification effect of stochastic resonance

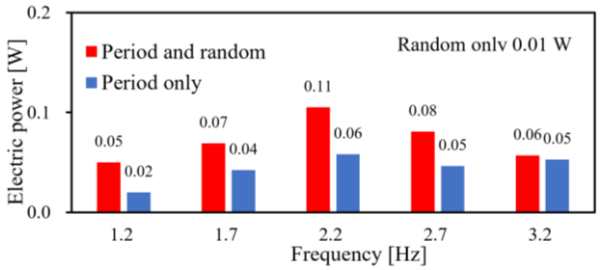

Fig. 18: Effect of liquid type when excited using Taft seismic wave

Figure 17 shows that when stochastic resonance occurred, the standard deviation of the response displacement of the mass block with respect to the support point is clearly larger than when stochastic resonance does not occur.

To quantitatively verify the amplification effect of stochastic resonance, two excitation approaches or methods, single and joint excitation, were used under similar input energy amounts. The sum of the standard deviations of the displacements obtained in separate random and periodic excitations was compared with that obtained in joint excitation.

When the periodic signal was 1.7 Hz, the sum of the standard deviations of the displacements obtained in separate excitation was 1.11+0.84 = 1.95 and the standard deviation of the displacement obtained in joint excitation was 2.83. The difference between both approaches was (2.83-1.95)/1.95 = 45.13%.

When the periodic signal was 2.2 Hz, the sum of the standard deviations of the displacements obtained in separate excitation was 1.11+0.62 = 1.73 and the displacement standard deviation obtained in joint excitation was 2.81. The difference between both approaches was (2.81-1.73)/1.73 = 62.43%.

When the periodic signal was 2.7 Hz, the sum of the standard deviations of the displacements obtained in separate excitation was 1.11+0.58 = 1.69 and the displacement standard deviation obtained in joint excitation was 3.31. The difference between both approaches was (3.31-1.69)/1.69 = 95.86%.

Therefore, using the two types of excitation signals, the relative standard deviation of the response displacement obtained in joint excitation was larger than that in individual excitation. This difference was attributed to the amplification effect caused by the stochastic resonance phenomenon.

Effect of Stochastic Resonance on Vibration Power Generation

The average of the generated electrical power for each measurement described in the previous section was calculated using Eq. (24) and the results are shown in Fig. 18.

Figure 18, the blue graph indicates the average electrical power under periodic excitation and the red graph indicates the average electrical power under joint excitation with random and periodic signals.

Figure 18 shows that the generated vibration power in the bistable vibration state was higher than that in the monostable motion state when stochastic resonance occurred.

In the case of joint excitation using random and a periodic signal of 1.7 Hz, the sum of the generated vibration power under separate excitation was 0.01+0.04 = 0.05 W, and that under joint excitation was 0.07 W. The difference between the two approaches was (0.07-0.05)/ 0.05 = 40.00 %.

In the case of joint excitation with a random signal and a periodic signal of 2.2 Hz, the sum of the generated vibration power under separate excitation was 0.01+0.06 = 0.07 W, and that under joint excitation was 0.11 W. The difference between the two approaches was (0.11-0.07)/ 0.07 = 57.14 %.

In the case of joint excitation with a random signal and a periodic signal of 2.7 Hz, the sum of the generated vibration power under separate excitation was 0.01+0.05 = 0.06 W, and that under joint excitation was 0.08 W. The difference between the two approaches was (0.08-0.06)/ 0.06 = 33.33 %.

These results indicate that the amount of power generated by joint excitation was larger than that generated by separate excitation using equal random and periodic excitation signals. It was confirmed that the power generation efficiency was improved because of the occurrence of stochastic resonance.

Conclusion

In this study, a horizontal bistable kinetic energy harvesting system using an electromagnetic motor was proposed and examined in detail and the following conclusions were obtained.

Based on the spring-mass bistable motion model, a vibration energy harvesting system was proposed by directly using an electromagnetic motor. The motion

governing equation of the mass block was established, which was the moving body of the vibration system. Its potential energy performance was analyzed and proven to have bistable vibration characteristics over the entire vibration range of the vibration system.

The frequency range of the periodic signal applied to generate stochastic resonance was investigated in order to expand the vibration amplitude. Using Kramer's rate, a frequency prediction formula for periodic signals prone to stochastic resonance was derived. The validity of the prediction formula was verified by comparing the predicted values and measurement results, which were found to be in good agreement.

In the excitation experiments, the proposed bistable vibrational energy harvesting system reliably generated stochastic resonance when random and periodic signals were co-excited. Furthermore, it was confirmed that there was a significant vibration amplification effect which substantially improved the vibration power generation performance.

For our future research, we intend to advance into the research and development phase to achieve the practical implementation of a bi-stable vibration energy harvesting system that harnesses the amplification effect of stochastic resonance.

Acknowledgment

We are grateful to all of those with whom we have had the pleasure to work during this and other related projects.

Funding Information

This research received no external funding.

Author's Contributions

Wei Zhao: Written original drafted preparation methodology.

Yoshiro Fujiwara: Data curation validation.

Jingchao Guan: Written reviewed and edited conceptualization.

Apollo B. Fukuchi: Investigation data curation.

Xilu Zhao: Written reviewed and edited investigation.

Ethics

The authors declare no ethical issues.

References

Ali, S. F., Adhikari, S., Friswell, M. I., & Narayanan, S. (2011). The analysis of piezomagnetoelastic energy harvesters under broadband random excitations. *Journal of Applied Physics*, *109*(7). https://doi.org/10.1063/1.3560523

Benzit, R., Sutera, A., & Vulpiani, A. (1981). The mechanism of stochastic resonance. *J. Phys. A: Math. Gen*, *14*, L453-L457. https://doi.org/10.1088/0305-4470/14/11/006

Bilgen, O., Friswell, M. I., Ali, S. F., & Litak, G. (2015). Broadband vibration energy harvesting from a vertical cantilever piezocomposite beam with tip mass. *International Journal of Structural Stability and Dynamics*, *15*(02), 1450038. https://doi.org/10.1142/S0219455414500382

Bouhedma, S., Zheng, Y., Lange, F., & Hohlfeld, D. (2019). Magnetic frequency tuning of a multimodal vibration energy harvester. *Sensors*, *19*(5), 1149. https://doi.org/10.3390/s19051149

Cao, J., Zhou, S., Wang, W., & Lin, J. (2015). Influence of potential well depth on nonlinear tristable energy harvesting. *Applied Physics Letters*, *106*(17). https://doi.org/10.1063/1.4919532

Chen, Z., He, J., & Wang, G. (2019). Vibration bandgaps of piezoelectric metamaterial plate with local resonators for vibration energy harvesting. *Shock and Vibration, 2019*. https://doi.org/10.1155/2019/1397123

Cottone, F., Basset, P., Vocca, H., Gammaitoni, L., & Bourouina, T. (2014). Bistable electromagnetic generator based on buckled beams for vibration energy harvesting. *Journal of Intelligent Material Systems and Structures*, *25*(12), 1484-1495. https://doi.org/10.1177/1045389X13508330

Dai, X. (2016). An vibration energy harvester with broadband and frequency-doubling characteristics based on rotary pendulums. *Sensors and Actuators A: Physical*, *241*, 161-168. https://doi.org/10.1016/j.sna.2016.02.004

Dong, L., Grissom, M., & Fisher, F. T. (2015). Resonant frequency of mass-loaded membranes for vibration energy harvesting applications. *AIMS Energy*, *3*(3), 344-359. https://doi.org/10.3934/energy.2015.3.344

Friswell, M. I., Ali, S. F., Bilgen, O., Adhikari, S., Lees, A. W., & Litak, G. (2012). Non-linear piezoelectric vibration energy harvesting from a vertical cantilever beam with tip mass. *Journal of Intelligent Material Systems and Structures*, *23*(13), 1505-1521. https://doi.org/10.1177/1045389X12455722

Gafforelli, G., Corigliano, A., Xu, R., & Kim, S. G. (2014). Experimental verification of a bridge-shaped, nonlinear vibration energy harvester. *Applied Physics Letters*, *105*(20). https://doi.org/10.1063/1.4902116

Gammaitoni, L. P. H., Anggi, P. Jung, F. Marchesoni. (1998). Stochastic resonance. *Rev. Mod. Phys*, *70*(1), 223-287. https://doi.org/10.1103/RevModPhys.70.223

Gammaitoni, L., Neri, I., & Vocca, H. (2009). Nonlinear oscillators for vibration energy harvesting. *Applied Physics Letters*, *94*(16). https://doi.org/10.1063/1.3120279

Gao, Y., Leng, Y., Javey, A., Tan, D., Liu, J., Fan, S., & Lai, Z. (2016). Theoretical and applied research on bistable dual-piezoelectric-cantilever vibration energy harvesting toward realistic ambience. *Smart Materials and Structures*, *25*(11), 115032. https://doi.org/10.1088/0964-1726/25/11/115032

Guo, L., Zhao, W., Gomi, N., Guan, J., & Zhao, X. (2022a). Development of an Opposed Mass-Spring Type Bi-Stable Vibration Energy Harvesting System Using Stochastic Resonance. *International Journal of Mechanical Engineering and Applications*, *10*(6), 123-134.

Guo, L., Zhao, W., Guan, J., Gomi, N., & Zhao, X. (2022b). Horizontal Bi-Stable Vibration Energy Harvesting Using Electromagnetic Induction and Power Generation Efficiency Improvement via Stochastic Resonance. *Machines*, *10*(10), 899. https://doi.org/10.3390/machines10100899

Harne, R. L., & Wang, K. W. (2013). A review of the recent research on vibration energy harvesting via bistable systems. *Smart Materials and Structures*, *22*(2), 023001. https://doi.org/10.1088/0964-1726/22/2/023001

Ibrahim, A., Towfighian, S., & Younis, M. I. (2017). Dynamics of transition regime in bistable vibration energy harvesters. *Journal of Vibration and Acoustics*, *139*(5), 051008. https://doi.org/10.1115/1.4036503

Khan, F. U., & Ahmad, I. (2016). Review of energy harvesters utilizing bridge vibrations. *Shock and Vibration*, *2016*. https://doi.org/10.1155/2016/1340402

Kubba, A. E., & Jiang, K. (2013). Efficiency enhancement of a cantilever-based vibration energy harvester. *Sensors*, *14*(1), 188-211. https://doi.org/10.3390/s140100188

Kumar, A., Sharma, A., Vaish, R., Kumar, R., & Jain, S. C. (2018). A numerical study on flexoelectric bistable energy harvester. *Applied Physics A*, *124*, 1-9. https://doi.org/10.1007/s00339-018-1889-6

Lallart, M., Anton, S. R., & Inman, D. J. (2010). Frequency self-tuning scheme for broadband vibration energy harvesting. *Journal of Intelligent Material Systems and Structures*, *21*(9), 897-906. https://doi.org/10.1177/1045389X10369716

Lan, C. B., & Qin, W. Y. (2014). Energy harvesting from coherent resonance of horizontal vibration of beam excited by vertical base motion. *Applied Physics Letters*, *105*(11). https://doi.org/10.1063/1.4895921

Lan, C., Tang, L., Qin, W., & Xiong, L. (2018). Magnetically coupled dual-beam energy harvester: Benefit and trade-off. *Journal of Intelligent Material Systems and Structures*, *29*(6), 1216-1235. https://doi.org/10.1177/1045389X17730927

Li, Y., Zhou, S., & Litak, G. (2020). Uncertainty analysis of bistable vibration energy harvesters based on the improved interval extension. *Journal of Vibration Engineering & Technologies*, *8*, 297-306. https://doi.org/10.1007/s42417-019-00134-z

Liu, W. Q., Badel, A., Formosa, F., Wu, Y. P., & Agbossou, A. (2013a). Novel piezoelectric bistable oscillator architecture for wideband vibration energy harvesting. *Smart Materials and Structures*, *22*(3), 035013. https://doi.org/10.1088/0964-1726/22/3/035013

Liu, W. Q., Badel, A., Formosa, F., Wu, Y. P., & Agbossou, A. (2013b). Wideband energy harvesting using a combination of an optimized synchronous electric charge extraction circuit and a bistable harvester. *Smart Materials and Structures*, *22*(12), 125038. https://doi.org/10.1088/0964-1726/22/12/125038

McNamara, B., & Wiesenfeld, K. (1989). Theory of stochastic resonance. *Physical review A*, *39*(9), 4854. https://doi.org/10.1103/PhysRevA.39.4854

Mei, X., Zhou, S., Yang, Z., Kaizuka, T., & Nakano, K. (2020a). A tri-stable energy harvester in rotational motion: Modeling, theoretical analyses and experiments. *Journal of Sound and Vibration*, *469*, 115142. https://doi.org/10.1016/j.jsv.2019.115142

Mei, X., Zhou, S., Yang, Z., Kaizuka, T., & Nakano, K. (2020b). A passively self-tuning nonlinear energy harvester in rotational motion: theoretical and experimental investigation. *Smart Materials and Structures*, *29*(4), 045033. https://doi.org/10.1088/1361-665X/ab78b2

Pellegrini, S. P., Tolou, N., Schenk, M., & Herder, J. L. (2013). Bistable vibration energy harvesters: a review. *Journal of Intelligent Material Systems and Structures*, *24*(11), 1303-1312. https://doi.org/10.1177/1045389X12444940

Podder, P., Amann, A., & Roy, S. (2015). Combined effect of bistability and mechanical impact on the performance of a nonlinear electromagnetic vibration energy harvester. *IEEE/ASME Transactions On Mechatronics*, *21*(2), 727-739. https://doi.org/10.1109/TMECH.2015.2451016

Rosas, A., & Lindenberg, K. (2016). Kramers' rate for systems with multiplicative noise. *Physical Review E*, *94*(1), 012101. https://doi.org/10.1103/PhysRevE.94.012101

Stephen, N. G. (2006). On energy harvesting from ambient vibration. *Journal of Sound and Vibration*, *293*(1-2), 409-425. https://doi.org/10.1016/j.jsv.2005.10.003

Tretyakov, M. V. (1998). Numerical technique for studying stochastic resonance. *Physical Review E*, *57*(4), 4789. https://doi.org/10.1103/PhysRevE.57.4789

Wang, K., Dai, X., Xiang, X., Ding, G., & Zhao, X. (2019). Optimal potential well for maximizing performance of bi-stable energy harvester. *Applied Physics Letters*, *115*(14). https://doi.org/10.1063/1.5095693

Yang, W., & Towfighian, S. (2017). A hybrid nonlinear vibration energy harvester. *Mechanical Systems and Signal Processing*, *90*, 317-333. https://doi.org/10.1016/j.ymssp.2016.12.032

Yao, C., Liu, Y., & Zhan, M. (2011). Frequency-resonance-enhanced vibrational resonance in bistable systems. *Physical Review E*, *83*(6), 061122. https://doi.org/10.1103/PhysRevE.83.061122

Zhang, H., Corr, L. R., & Ma, T. (2018a). Issues in vibration energy harvesting. *Journal of Sound and Vibration*, *421*, 79-90. https://doi.org/10.1016/j.jsv.2018.01.057

Zhang, X., Yang, W., Zuo, M., Tan, H., Fan, H., Mao, Q., & Wan, X. (2018b). An arc-shaped piezoelectric bistable vibration energy harvester: Modeling and experiments. *Sensors*, *18*(12), 4472. https://doi.org/10.3390/s18124472

Zhang, Y., Zheng, R., Kaizuka, T., Su, D., Nakano, K., & Cartmell, M. P. (2015). Broadband vibration energy harvesting by application of stochastic resonance from rotational environments. *The European Physical Journal Special Topics*, *224*, 2687-2701. https://doi.org/10.1140/epjst/e2015-02583-7

Zhao, W., Wu, Q., Zhao, X., Nakano, K., & Zheng, R. (2020). Development of large-scale bistable motion system for energy harvesting by application of stochastic resonance. *Journal of Sound and Vibration*, *473*, 115213. https://doi.org/10.1016/j.jsv.2020.115213

Zhao, W., Zheng, R., Yin, X., Zhao, X., & Nakano, K. (2022a). An Electromagnetic Energy Harvester of Large-Scale Bistable Motion by Application of Stochastic Resonance. Journal of Vibration and Acoustics, 144(1), 011007. https://doi.org/10.1115/1.4051265

Zhao, W., Zhang, X., Kawada, N., & Zhao, X. (2022b). A Magnet-Coil-Type Bistable Vibration Energy Harvester for Random Wave Environment. *Shock and Vibration*, *2022*. https://doi.org/10.1155/2022/3552941

Zheng, R., Nakano, K., Hu, H., Su, D., & Cartmell, M. P. (2014). An application of stochastic resonance for energy harvesting in a bistable vibrating system. *Journal of Sound and Vibration*, *333*(12), 2568-2587. https://doi.org/10.1016/j.jsv.2014.01.020

Zhou, S., Cao, J., Wang, W., Liu, S., & Lin, J. (2015). Modeling and experimental verification of doubly nonlinear magnet-coupled piezoelectric energy harvesting from ambient vibration. *Smart Materials and Structures*, *24*(5), 055008. https://doi.org/10.1088/0964-1726/24/5/055008

Zou, H. X., Zhang, W. M., Li, W. B., Hu, K. M., Wei, K. X., Peng, Z. K., & Meng, G. (2017). A broadband compressive-mode vibration energy harvester enhanced by magnetic force intervention approach. *Applied Physics Letters*, *110*(16). https://doi.org/10.1063/1.4981256

Zou, H. X., Zhang, W. M., Li, W. B., Wei, K. X., Hu, K. M., Peng, Z. K., & Meng, G. (2018). Magnetically coupled flextensional transducer for wideband vibration energy harvesting: Design, modeling and experiments. *Journal of Sound and Vibration*, *416*, 55-79. https://doi.org/10.1016/j.jsv.2017.11.041

Zuo, L., & Tang, X. (2013). Large-scale vibration energy harvesting. *Journal of Intelligent Material Systems and Structures*, *24*(11), 1405-1430. https://doi.org/10.1177/1045389X13486707